

# **COMPUTER SIMULATION FOR COMBUSTION AND EXHAUST EMISSIONS IN SPARK IGNITION ENGINE FUELED WITH ETHANOL**

Maher Abdul-Resul Sadiq Al-Baghdadi\*

Department of Mechanical Engineering, The Higher Center for  
Engineering Comprehensive Vocations, Yefren, Libya



## **Address**

Maher Abdul-Resul Sadiq Al-Baghdadi  
The Higher Center for Engineering Comprehensive Vocations.  
P.O. Box 65943  
Fax: 00218-21-3602362  
E-mail address: [maherars@hotmail.com](mailto:maherars@hotmail.com)  
Yefren,  
Libya.

## ABSTRACT

Computer simulations of internal combustion engine cycles are desirable because of the aid they provide in design studies, in predicting trends, in serving as diagnostic tools, in giving more data than are normally obtainable from experiments, and in helping to understand the complex processes that occur in the combustion chamber.

A computer quasi-one dimensional model simulating the compression, combustion and expansion processes of the spark ignition engine cycles with all exhaust emissions have been developed for ethanol fuel.

A system of first order ordinary differential equations were obtained for the pressure, mass, volume, temperature of the burned and unburned gases, heat transfer from burned and unburned zone, mass flow into and out of crevices and the composition of combustion products.

The results obtained from the present studies have shown the capability of the model to predict satisfactorily the performance and emissions of a spark ignition engine fueled with ethanol fuel.

**Keywords:** Computer simulation; Power generation; Pollution; ICE; Spark ignition engine model; Mathematical model; Thermodynamics; Ethanol fuel.

## NOMENCLATURE

A	Cylinder heat transfer area.	P <sub>0</sub>	Reference pressure.
[Air]	Molar concentration of the air.	R <sub>mol</sub>	Universal gas constant
[E]	Molar concentration of the ethanol fuel.	rpm	Engine speed.
Ac	Surface chamber in contact with (Ven)	S	Stroke.
A <sub>fl</sub>	Flame front area.	ST	Turbulent flame front speed.
ar	Crank radius.	T	Gas temperature.
B	Cylinder bore.	T <sub>b</sub>	Gas temperature of burned zone.
C <sub>p</sub>	Specific heat at constant pressure.	T <sub>0</sub>	Reference temperature.
C <sub>v</sub>	Specific heat at constant volume.	T <sub>u</sub>	Gas temperature of unburned zone.
D <sub>p</sub>	Delay period.	T <sub>w</sub>	Cylinder temperature.
E	Internal energy.	U <sub>p</sub>	Mean piston speed.
K	Thermal conductivity.	v	Specific volume.
K <sub>P</sub>	Equilibrium constant.	V <sub>c</sub>	Clearance volume.
L	Distance between crank axis and piston pin axis	V <sub>cyl</sub>	Cylinder volume.
M	Cylinder total mass.	V <sub>en</sub>	Enflamed volume.
M <sub>b</sub>	Mass of burned gases.	X <sub>f</sub>	Mole fraction of fresh mixture
M <sub>u</sub>	Mass of unburned gases.	X <sub>R</sub>	Mole fraction of residual gas.
MW <sub>b</sub>	Molecular weight of burned gas mixture.	<b>q</b>	Crank angle.
MW <sub>u</sub>	Molecular weight of unburned gas mix.	<b>m</b>	Kinematics gas viscosity.
N	Number of mole.	<b>r</b>	Density of gas mixture.
N <sub>cr</sub>	Number of mole in crevice.	<b>Dq</b>	Crank angle step.
P	Cylinder pressure.	<b>f</b>	Equivalence ratio.
		<b>d</b>	Stefan-Boltzman constant = 5.67e <sup>-8</sup>

## **1- INTRODUCTION**

Considering energy crises and pollution problems today, investigations have been concentrated on decreasing fuel consumption by using alternative fuels and on lowering the concentration of toxic components in combustion products. One of the major areas of development in the internal combustion engine is the development of computer simulations of various types of engines. Their economic value is in the reduction in time and costs for the development of new engines and their technical value is in the identification of areas, which require specific attention as the design study evolves. Computer simulations of internal combustion engine cycles are desirable because of the aid they provide in design studies, in predicting trends, in serving as diagnostic tools, in giving more data than are normally obtainable from experiments, and in helping to understand the complex processes that occur in the combustion chamber. In the present work a quasi one-dimensional model was developed to simulate a four-stroke cycle of a spark ignition engine fueled with ethanol fuels.

## **2- AVAILABILITY AND SUITABILITY OF ALCOHOL AS AN S.I. ENGINE FUEL**

Alcohol fuels are made from renewable resources like locally grown crops and even waste products such as waste paper or grass and tree trimmings. Alcohol is a likely alternative automotive fuel in that it has properties, which would allow its use in present engines with minor modifications. It has a high octane number than gasoline. A fuel with a higher-octane level can endure a higher compression rate before exploding, giving the engine the ability of delivering more power and thus being more powerful and economical. Alcohol fuels burn cleaner than regular gasoline and produce less carbon monoxide and nitrogen oxides. Alcohol fuel has high heat of vaporization, therefore, it is reduce the peak temperature inside the cylinder and hence reduce the NOx emissions and increase the engine power.

### 3- MODELING OF THE SPARK IGNITION ENGINE

The combustion chamber was generally divided into burned and unburned zones separated by a flame front (figure 1). The first law of thermodynamic, equation of state and conservation of mass and volume were applied to the burned and unburned zones. The pressure was assumed to be uniform throughout the cylinder charge. A system of first order ordinary differential equations were obtained for the pressure, mass, volume, temperature of the burned and unburned zones, heat transfer from burned and unburned zone, and mass flow into and out of crevices.

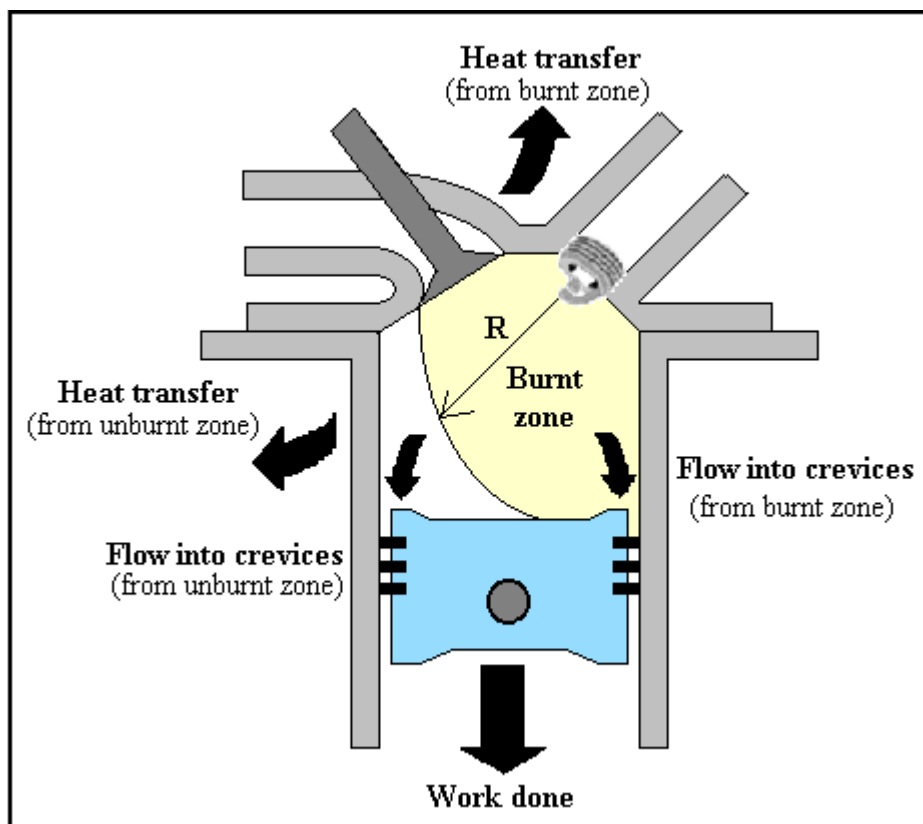


Figure 1: Two zone thermodynamic model of combustion.

The mass burning rate was modeled by the following equation [1];

$$\frac{dM_b}{dt} = A_{fl} \cdot r \cdot ST \quad \dots (1)$$

The turbulent flame front speed (ST) was modeled by the following semi-empirical formula;

$$\begin{aligned}
 ST = & (36.9 - 140.5(f - 1.11)) \times \left( \frac{T_u}{T_0} \right)^{2.18-0.8(f-1)} \times \left( \frac{P}{P_0} \right)^{0.16+0.22(f-1)} \times (1 - 2.06 \times R^{0.77}) \\
 & \times (1 + 0.0018 \text{ rpm}) \times \left( \frac{(r_u/r_b)}{(((r_u/r_b) - 1) \times b + 1)} \right) \\
 \dots (2)
 \end{aligned}$$

The following formula was used to calculate the equivalence ratio;

$$f = \frac{\left( \frac{[E]}{\text{Air}} \right)_{\text{Act.}}}{\left( \frac{[E]}{[\text{Air}]} \right)_{\text{St.}}} \dots (3)$$

The flame front area (A<sub>f</sub>) calculations were based on Annand model [3]. Figure (2) shows the geometry of the combustion chamber of diameter (B), height (h), with flame front radius (R), the spark location (a) from the edge and (0.5B-a) from the center and the areas of the chamber surface in contact with the enflamed material are C<sub>1</sub>, C<sub>2</sub>, and C<sub>3</sub>.

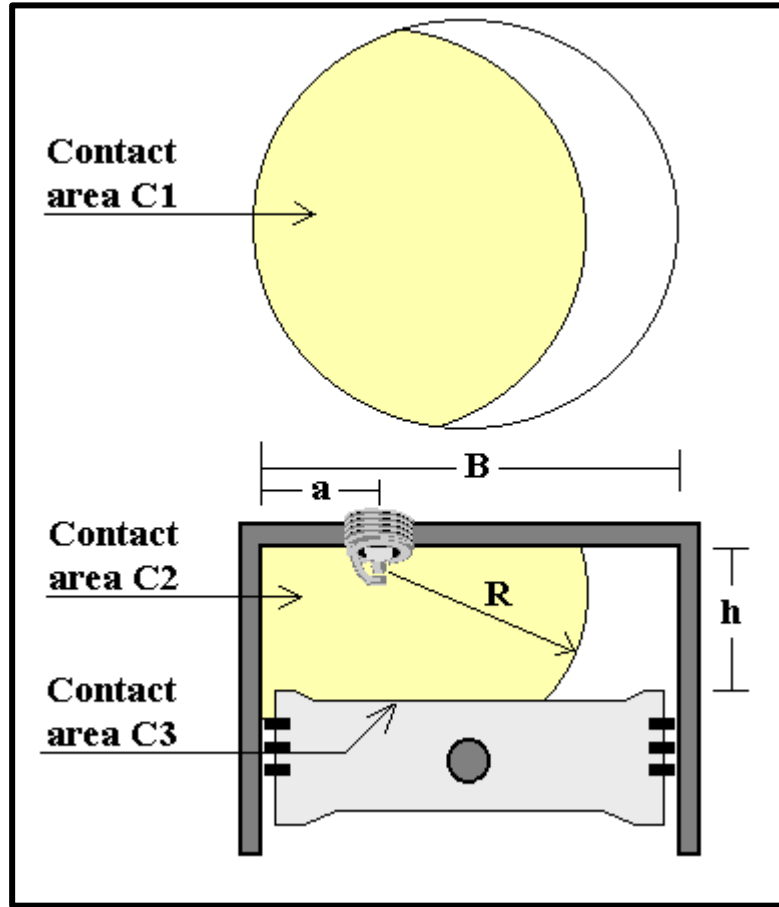


Figure 2: Basic geometry

The parameters to be determined are the enflamed volume ( $V_{en}$ ), the flame front area ( $A_{fl}$ ), and the area ( $A_c$ ) of the chamber surface in contact with the enflamed volume. It is convenient to divide ( $A_c$ ) into three areas ( $C_1$ ) on the upper flat surface, ( $C_2$ ) on the cylindrical wall, and ( $C_3$ ) on the lower flat surface. Let  $X_0$  be a variable such that  $X_0=R$  if  $R \leq h$ , otherwise  $X_0=h$ . The following cases are considered.

### Case 1: $R \leq a$

When flame front radius is less than or equal to the spark location distance ( $a$ ), all parameters are easily evaluated:

$$V_{en} = pX_0 \left( R^2 - \frac{X_0^2}{3} \right) \quad \dots (4)$$

$$A_{fl} = 2pR \cdot X_0 \quad \dots (5)$$

$$C1 = pR^2 \dots (6)$$

$$C2 = 0 \dots (7)$$

$$C3 = p(R^2 + X_0^2) \dots (8)$$

$$A_c = C1 + C2 + C3 \dots (9)$$

### Case 2: $R > a$

When flame front radius is greater than spark location distance ( $a$ ), the calculation becomes more complex, and another parameter may be defined.

The intersection of the flame front and the curved chamber wall with a plane parallel to the flat face, at distance ( $Y$ ) from the upper is shown in figure (3).

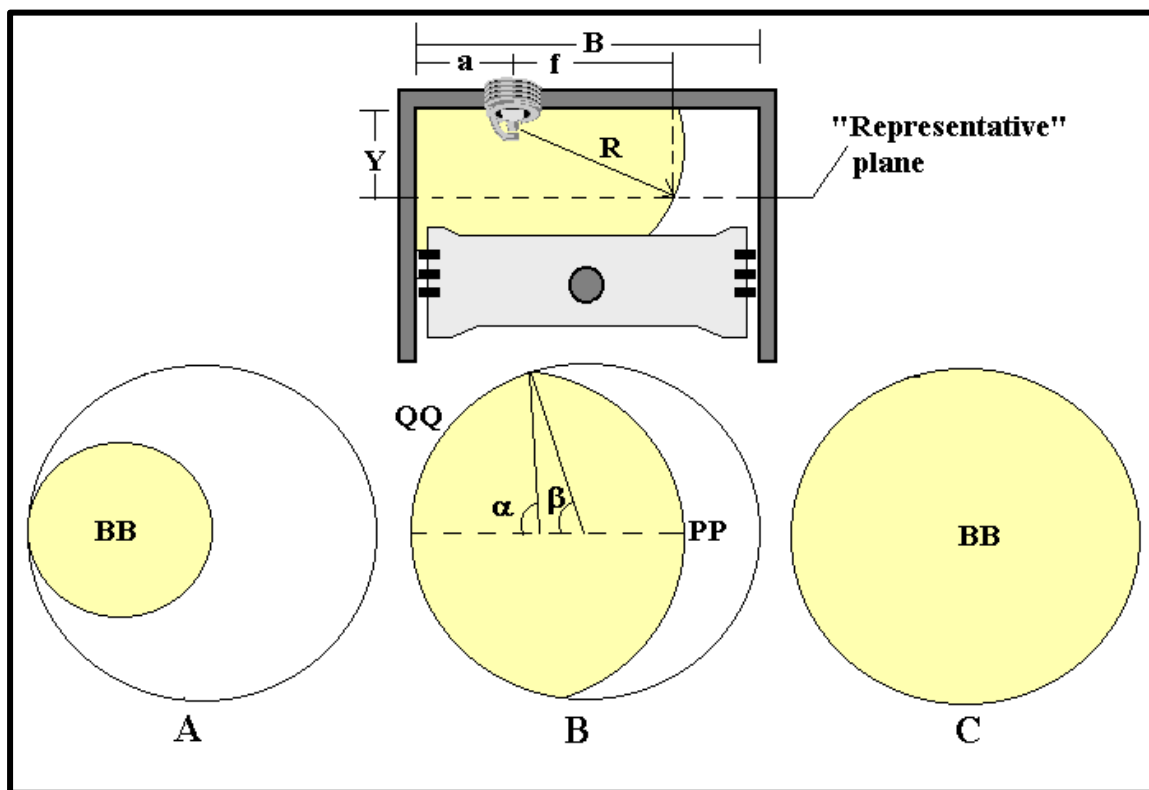


Figure 3: Flame front radius is greater than spark location distance

wall contact by (QQ). Let (f) is defined as a radius of intersection of flame front with plane (Y) and is given by the following equation;

$$f = \sqrt{(R^2 + Y^2)} \quad \dots (10)$$

contact (QQ) the following three cases, depending on the value of (f), may be considered.

**When  $f \leq a$  (figure 3-A)**

$$BB = p \cdot f^2 \quad \dots (11)$$

$$PP = 2p \cdot f \quad \dots (12)$$

$$QQ = 0 \quad \dots (13)$$

**When  $a < f < (B-a)$ , (figure 3-B)**

The angle  $\alpha$  and  $\beta$  which are defined in figure (3-B), are given by;

$$\cos(a) = \left[ \left( \frac{a}{B} - \left( \frac{a}{B} \right)^2 - \left( \frac{f}{B} \right)^2 \right) \right] \left/ \left( \frac{(1-2a)f}{B} \right) \right. \quad \dots (14)$$

$$\cos(b) = \left[ 1 + \left( \left( \frac{a}{B} \right)^2 - \left( \frac{f}{B} \right)^2 \right) \right] \left/ \left( \frac{1}{2} - \frac{a}{B} \right) \right. \quad \dots (15)$$

then,

$$BB = \left[ \left( p - a + \frac{1}{2} \sin(2a) \right) f^2 + (2b - \sin(2b)) \left( \frac{B^2}{8} \right) \right] \quad \dots (16)$$

$$PP = 2f(p - B) \quad \dots (17)$$

$$QQ = B \cdot b \quad \dots (18)$$

**When  $f \geq (B-a)$ , (figure 3-C)**

$$BB = \frac{pB^2}{4} \quad \dots (19)$$

$$PP = 0 \quad \dots (20)$$

$$QQ = p \cdot a \quad \dots (21)$$

Three ranges are recognized during case 2 (i.e.  $R > a$ ), which are shown in figure (4);

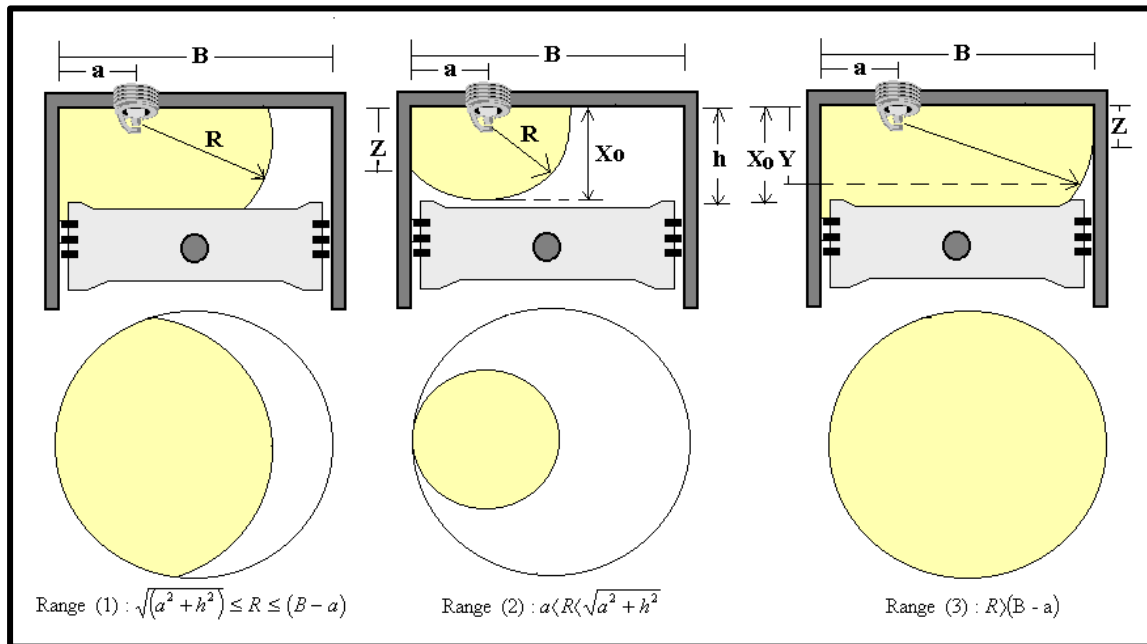


Figure 4: The three ranges of case 2

Range (1): In this range the set of equations suggested by Annand [3] be used;

$$Y = 0.58 X_o \quad \dots (22)$$

$$V_{en} = BB \cdot X_o \quad \dots (23)$$

$$A_{fl} = \frac{R \cdot P \cdot P}{f} \cdot X_o \quad \dots (24)$$

$$C_1 = BB \quad \dots (25)$$

$$C_2 = QQ \cdot X_o \quad \dots (26)$$

$$C_3 = BB \quad \dots (27)$$

$$AC = C_1 + C_2 + C_3 \quad \dots (28)$$

Range 2: In this range, it is necessary to divided the enflamed zone into two regions, above and below the intersection of the flame with the cylindrical wall, as indicated in figure (4), and the following set of equations are used;

$$Z = \sqrt{(R^2 - a^2)} \quad \dots (29)$$

$$Y = 0.58Z \quad \dots (30)$$

$$Ven = [BB.Z + p(Xo - Z)(R^2 - (Xo^2 + Xo.Z + Z^2))/3] \quad \dots (31)$$

$$Afl = \frac{R.PP.Z}{f} + 2p.R(Xo - Z) \quad \dots (32)$$

$$C1 = BB \quad \dots (33)$$

$$C2 = QQ.Z \quad \dots (34)$$

$$C3 = 0 \quad \dots (35)$$

$$AC = C1 + C2 + C3 \quad \dots (36)$$

Range 3: In this range, the enflamed zone is divided as in figure (4). If (Z) represent the depth at which the flame just touches the most remote point on the cylindrical wall, then the following set of equations are used;

$$Z = \sqrt{R^2 - (B - a)^2} \quad \dots (37)$$

$$Y = Z + 0.5(Xo - Z) \quad \dots (38)$$

$$Ven = \frac{p}{4} B^2 Z + BB(Xo - Z) \quad \dots (39)$$

$$Afl = \frac{PP.R.(Xo - Z)}{f} \quad \dots (40)$$

$$C1 = \frac{p.B^2}{4} \quad \dots (41)$$

$$C2 = p.BB.Z + QQ.(Xo - Z) \quad \dots (42)$$

$$C3 = BB \quad \dots (43)$$

$$AC = C1 + C2 + C3 \quad \dots (44)$$

The total cylinder volume at any crank angle position is given by Heywood [1] as;

$$V(q) = \left[ Vc + \left( \frac{Vcyl - Vc}{2} \right) \left( \frac{L}{ar} + 1 + \cos(q) - \sqrt{\left( \frac{L}{ar} \right)^2 - \sin^2(q)} \right) \right] \quad \dots (45)$$

The instantaneous heat interaction between the cylinder content (burned and unburned zones) and its walls was calculated by using the semi-empirical expression for a four stroke engine [1];

$$-\frac{dQ_{ht}}{dt} = A \left[ 0.26 \frac{k}{B} \left( \frac{Up \cdot B}{m} \right)^{0.7} (T - T_w) + 0.69s(T^4 - T_w^4) \right] \quad \dots (46)$$

The crevices are the volume between the piston, piston rings and cylinder wall (figure 1). Gases flow into and out of these volumes during the engine operating cycle as the cylinder pressure changes. The instantaneous energy flows to the crevices was calculated by using the semi-empirical expression of Gatowski et al. [5] for a spark ignition engine;

$$\frac{dQ_{cr}}{dq} = (e + R_{mol} \cdot T) \cdot \frac{dN_{cr}}{dq} \quad \dots (47)$$

where  $dN_{cr} > 0$  when flow is out of the cylinder into the crevice;  $dN_{cr} < 0$  when flow is from the crevice to the cylinder; and  $(e + R_{mol} \cdot T)$  is evaluated at cylinder conditions when  $dN_{cr} > 0$ , and at crevice conditions when  $dN_{cr} < 0$ .

In a conventional spark ignition engine the fuel and air are mixed together in the intake system, inducted through the intake valve into the cylinder, where mixing with residual gas takes place, and then compressed. Under normal operating conditions, combustion is initiated towards the end of the compression stroke at the spark plug by an electric discharge. Following inflammation, a turbulent flame develops, propagates through this essentially premixed fuel, air, burned gas mixture until it reaches the combustion chamber walls, and then extinguishes to begin expansion stroke until the exhaust valve opening. Each of these processes is discussed below to complete engine power cycle simulation.

The compression process starts at the trapped condition, and ends after delay period process, when the mixture is ignited by the spark plug. The state of the gas during this stage is derived by using a perfect mixing model for fresh charge and residuals from the previous cycle.

The first law of thermodynamics for an open system is;

$$\frac{dQ_{ht}}{dq} = N \cdot Cv \cdot \frac{dT}{dq} + p \frac{dV}{dq} + \frac{dQ_{cr}}{dq} \quad \dots (48)$$

The equation of state is ;

$$P \cdot V = N \cdot R_{mol} \cdot T \quad \dots (49)$$

A combination of equations (48) and (49) after rearrangement gives;

$$\frac{dP}{dq} = \left[ -\left( 1 + \frac{R_{mol}}{Cv} \right) P \cdot \frac{dV}{dq} - \frac{R_{mol}}{Cv} \cdot \frac{dQ_{cr}}{dq} + \frac{R_{mol}}{Cv} \cdot \frac{dQ_{ht}}{dq} \right] / V \quad \dots (50)$$

and

$$\frac{dT}{dq} = T \left( \frac{1}{P} \cdot \frac{dP}{dq} + \frac{1}{V} \cdot \frac{dV}{dq} \right) \quad \dots (51)$$

As the compression process continues the variable are incremented by using the following general expression;

$$X_{n+1} = X_n + \frac{dX}{dq} \cdot dq \quad \dots (52)$$

where X is any variable.

The numerical method used for this purpose is the Runge-Kutta method.

After spark occurrence, the delay period is calculated using the following equation;

$$DP = \left[ \left( \frac{6 \cdot rpm}{ST} \right) \sqrt[3]{\frac{0.001V_{cyl.}}{p}} \right] \quad \dots (53)$$

During this period the mixture is considered to be unburned and the compression process is continued. The process continues for as many time intervals as necessary until the total angle from the nominal spark timing is greater than delay period. The combustion process is said to have commenced, and is divided into two stages. The first stage is ignition and initiation of two zones in combustion space and the second stage is flame front propagation.

After the combustion of the small nucleus of fuel-air mixture the combustion chamber is subdivided into two zones, a burned zone, suffix (b), and an unburned zone, suffix (u).

The process is initiated in three steps A, B and C as shown in figure (5)[6];

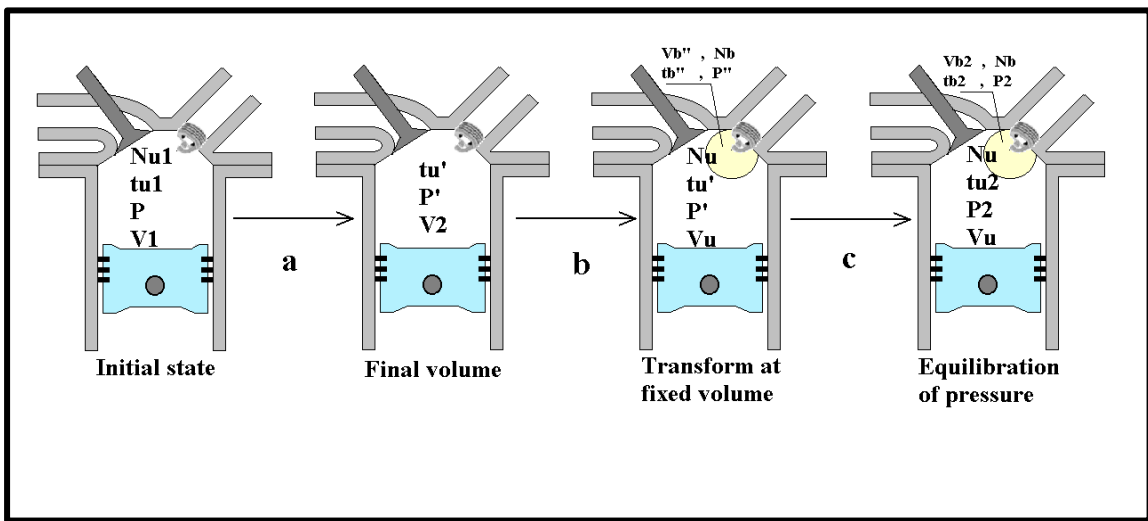


Figure 5: Basis of the first combustion stage calculation

**Step (A): End of delay period.**

The temperature and pressure inside the cylinder at the end of delay period are taken to be  $(tu')$  and  $(P')$ .

**Step (B): Appearance of flame nucleus.**

The mixture (at state  $P'$ ,  $tu'$ ) is assumed to burn adiabatically at constant volume to the product temperature,  $(tb'')$ . For this purpose an internal energy balance is made for a unit mass of the mixture. The first estimate of the product temperature  $(tb'')$  is based on the following expression;

$$tb'' = tu' + 2500 f \cdot X_f \quad \text{for } f \leq 1.0 \quad \dots (54)$$

and

$$tb'' = tu' + 2500 f \cdot X_f - 700(f-1) \cdot X_f \quad \text{for } f > 1.0 \quad \dots (55)$$

An energy balance is made and  $tb''$  adjusted by Newton Raphson method until the specific internal energy of the products equal to the specific internal energy of the reactions.

$$f(tb'') = E_b - E_u = 0 \quad \dots (56)$$

$$[tb'']_{n+1} = [tb'']_n - \frac{f(tb'')}{Nb \cdot C_{vb}} \quad \dots (57)$$

During this process ( $t_u'$ ) and ( $P'$ ) are kept unchanged. Using ( $t_b''$ ) as the product temperature for adiabatic constant volume combustion, ( $P''$ ) is calculated by the following equation;

$$P'' = \left[ \frac{Nb \cdot t_b''}{Nu \cdot t_u'} \right] \cdot P' \quad \dots (58)$$

To obtain the mass of the products ( $M_b$ ) at this stage, Benson et. al.[6] assume a slight increase in the density of the products compared with the density of the mixture, and he showed after many experimental and from large number of calculations that;

$$M_b = \frac{2pR^3 \cdot M}{3V_{cyl}} + 2e^{-10} \cdot \frac{M}{V_{cyl}} \quad \dots (59)$$

Now

$$M_u = M - M_b \quad \dots (60)$$

And

$$V_u = \frac{M_u}{M} \cdot V_2 \quad \dots (61)$$

So that the total internal energy is;

$$E = Nu \cdot eu + Nb \cdot eb \quad \dots (62)$$

### **Step (C): Equilibration of pressure.**

This step is assumed to be an adiabatic constant volume process. The total internal energy is;

$$E = Nu \cdot eu + Nb \cdot eb \quad \dots (63)$$

Balancing the total internal energy before and after step (C);

$$Nu \cdot eu + Nb \cdot eb = Nu \cdot eu + Nb \cdot eb \quad \dots (64)$$

Which, after rearrangement, becomes;

$$Nu \cdot C_{vu} \cdot t_u' \left( \frac{t_u^2}{t_u'} - 1 \right) = Nb \cdot C_{vb} \left( 1 - \frac{t_b^2}{t_b''} \right) \quad \dots (65)$$

As before;

$$\frac{t_u^2}{t_u'} = \left( \frac{P^2}{P'} \right)^{\frac{(K_u - 1)}{K_u}} \quad \dots (66)$$

$$\frac{tb2}{tb''} = \left( \frac{P2}{P''} \right)^{\frac{(Kb-1)}{Kb}} \quad \dots (67)$$

Where;

$$Ku = \frac{C_{pu}}{C_{vu}} \quad \dots (68)$$

$$Kb = \frac{C_{pb}}{C_{vb}} \quad \dots (69)$$

Now from equation of state;

$$\frac{P2}{P''} = \frac{P2}{P'} \cdot \frac{P'}{P''} = \frac{P2}{P'} \cdot \frac{Ru}{Rb} \cdot \frac{tu'}{tb''} \quad \dots (70)$$

Combination equation (65), (67) and (70), and assuming that;

$$\frac{tu2}{tu'} = ZZ \quad \dots (71)$$

$$\frac{Ku}{Ku-1} \cdot \frac{Kb-1}{Kb} = KK \quad \dots (72)$$

$$\frac{Nb \cdot Cv_b \cdot tb''}{Nu \cdot 2 \cdot Cv_u \cdot tu'} = SS \quad \dots (73)$$

$$\frac{Ru \cdot tu'}{Rb \cdot tb''} = GG \quad \dots (74)$$

Then;

$$ZZ - 1 = SS(1 - GG \cdot ZZ^{KK}) \quad \dots (75)$$

Which is solved for (ZZ) by an iterative technique. Then cylinder pressure is calculated from equation (66).

The cylinder pressure and the temperature of burned and unburned zones of the flame front propagation stage were modeled as shown below;

The first law of thermodynamics for an open system is;

$$\frac{dQ_{ht}}{dq} = \frac{dE}{dq} + P \cdot \frac{dV}{dq} + \frac{dQ_{cr}}{dq} \quad \dots (76)$$

The total internal energy of cylinder contents is;

$$E = Eb + Eu = Nb \cdot eb + Nu \cdot eu \quad \dots (77)$$

Therefor,

$$\frac{dE}{dq} = Nb \cdot \frac{deb}{dq} + eb \cdot \frac{dNb}{dq} + Nu \cdot \frac{deu}{dq} + eu \cdot \frac{dNu}{dq} \quad \dots (78)$$

and

$$MWb \cdot \frac{dNb}{dq} = -MWu \cdot \frac{dNu}{dq} \quad \dots (79)$$

Therefore, equation (78) becomes

$$\frac{dE}{dq} = \left[ \left( eb - eu \cdot \frac{MWb}{MWu} \right) \frac{dNb}{dq} + Nb \cdot Cv \cdot \frac{dTb}{dq} + Nu \cdot Cv \cdot \frac{dTu}{dq} \right] \quad \dots (80)$$

The cylinder volume at each time step is;

$$\frac{dV}{dq} = \frac{dVu}{dq} + \frac{dVb}{dq} \quad \dots (81)$$

and differentiating the equation of state ( $P \cdot V = N \cdot R \cdot mol \cdot T$ ),

$$\frac{dV}{dq} = \left[ \left( \frac{Vb}{Nb} - \frac{Vu}{Nu} \cdot \frac{MWb}{MWu} \right) \frac{dNb}{dq} + \frac{Nu \cdot R \cdot mol}{P} \cdot \frac{dTu}{dq} + \frac{Nb \cdot R \cdot mol}{P} \cdot \frac{dTb}{dq} - \frac{V}{P} \cdot \frac{dP}{dq} \right] \quad \dots (82)$$

Applying the first law to a unit mole for unburned zone;

$$\frac{deu}{dq} = \frac{1}{Nu} \cdot \frac{dQht,u}{dq} - P \cdot \frac{dvu}{dq} - \frac{1}{Nu} \cdot \frac{dQcr,u}{dq} \quad \dots (83)$$

and

$$\frac{deu}{dq} = Cv \cdot \frac{dTu}{dq} \quad \dots (84)$$

Differentiating the equation of state for a unit mole of unburned zone gives;

$$\frac{dvu}{dq} = \frac{R \cdot mol}{P} \cdot \frac{dTu}{dq} - \frac{vu}{P} \cdot \frac{dP}{dq} \quad \dots (85)$$

The combination of equations (83), (84) and (85) for ( $Nu$ ) moles of unburned mixture after rearrangement gives;

$$\frac{dTu}{dq} = \frac{1}{Nu \cdot Cpu} \cdot \frac{dQht,u}{dq} + \frac{Vu}{Nu \cdot Cpu} \cdot \frac{dP}{dq} - \frac{1}{Nu \cdot Cpu} \cdot \frac{dQcr,u}{dq} \quad \dots (86)$$

A combination of equations (82) and (86) after rearrangement gives;

$$\frac{dTb}{dq} = \frac{P}{Nb \cdot R \cdot mol} \left[ \frac{dV}{dq} - \left( \frac{R \cdot mol \cdot Tb}{P} - \frac{R \cdot mol \cdot Tu}{P} \cdot \frac{MWb}{MWu} \right) \frac{dNb}{dq} - \frac{Vu \cdot R \cdot mol}{P \cdot Cpu} \cdot \frac{dP}{dq} - \frac{R \cdot mol}{P \cdot Cpu} \cdot \frac{dQht,u}{dq} + \frac{R \cdot mol}{P \cdot Cpu} \cdot \frac{dQcr,u}{dq} + \frac{V}{P} \cdot \frac{dP}{dq} \right] \quad \dots (87)$$

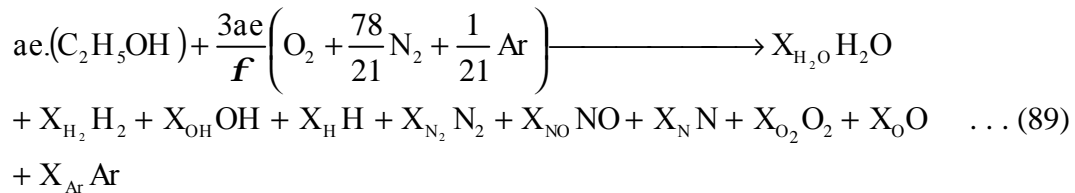
Finally a combination of equations (76), (80), (86) and (87) after rearrangement gives;

$$\frac{dP}{dq} = \left[ \frac{\left[ p \frac{dV}{dq} \left( 1 + \frac{Cvb}{Rmol} \right) + \left( \frac{Cvu}{Cpu} - \frac{Cvb}{Cpu} \right) \frac{dQht,u}{dq} + \left( eb - eu \cdot \frac{MWb}{MWu} \right) \frac{dNb}{dq} \right]}{\left[ \frac{Cvu}{Cpu} \cdot Vu - \frac{Cvb}{Cpu} \cdot Vu + \frac{Cvb}{Rmol} \cdot V \right]} \right. \\ \left. - \left( Cvb \left( Tb - Tu \cdot \frac{MWb}{MWu} \right) \right) \frac{dNb}{dq} + \left( \frac{Cvb}{Cpu} - \frac{Cvu}{Cpu} \right) \frac{dQcr,u}{dq} + \frac{dQcr}{dq} - \frac{dQht}{dq} \right] \right] \quad \dots (88)$$

Equations (86), (87) and (88) are solved by Runge-Kutta method to calculate the unburned zone temperature, the burned zone temperature and the cylinder pressure respectively during each time step.

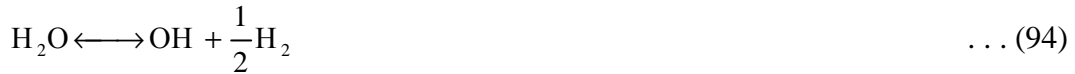
Once the combustion is complete the variables are organized to calculate for single zone only. The Runge-Kutta method is used. Throughout the expansion calculation a check is kept to see if NO is frozen when the NO rate kinetic calculations are by-passed.

Ten species were considered in the calculation of combustion product concentrations. The calculation starts from the equation of combustion of ethanol fuels and air, which is represented by;



The composition was calculated in terms of molar fractions of these species denoted by  $X_i$ . The equilibrium distribution of these species can be fully described by the following six reactions;





The equilibrium constants for these reactions are;

$$\text{KP 1} = \frac{X_{\text{H}}}{\sqrt{X_{\text{H}_2}}} \cdot \sqrt{P} \quad \dots (97)$$

$$\text{KP 2} = \frac{X_{\text{O}}}{\sqrt{X_{\text{O}_2}}} \cdot \sqrt{P} \quad \dots (98)$$

$$\text{KP 3} = \frac{X_{\text{N}}}{\sqrt{X_{\text{N}_2}}} \cdot \sqrt{P} \quad \dots (99)$$

$$\text{KP 4} = \frac{X_{\text{O}_2}}{b^2} \cdot P \quad \dots (100)$$

$$\text{KP 5} = \frac{X_{\text{OH}}}{b \cdot \sqrt{X_{\text{H}_2}}} \cdot \sqrt{P} \quad \dots (101)$$

$$\text{KP 6} = \frac{b \cdot X_{\text{CO}}}{X_{\text{CO}_2}} \quad \dots (102)$$

$$\text{KP 7} = \frac{X_{\text{NO}}}{b \cdot \sqrt{X_{\text{N}_2}}} \cdot \sqrt{P} \quad \dots (103)$$

$$\text{where } b = \frac{X_{\text{H}_2\text{O}}}{X_{\text{H}_2}} \quad \dots (104)$$

There are 13 unknowns in equation (89), namely 12 mole fractions  $X_i$  and the total number of moles of fuel (ae). Seven equations are available (97-103), therefore six more equations are needed for the solution.

One of these is;

$$\sum_{i=1}^{i=12} X_i = 1 \quad \dots (105)$$

The reminders are the atomic balances for Argon, Hydrogen, Oxygen, and Nitrogen.

Let the number of atoms of Ar, H, O and N corresponding to 1 mole of fuel by VE, XE, LE, and ZE respectively, and noting that (ae) moles of fuel corresponding to 1 mole of productions.

The following atomic balance can be made as follows;

$$\text{Argon: } X_{\text{Ar}} = \text{ae.VE} \quad \dots (106)$$

$$\text{Carbon: } X_{\text{CO}} + X_{\text{CO}_2} = \text{ae.WE} \quad \dots (107)$$

$$\text{Hydrogen: } 2X_{\text{H}_2\text{O}} + 2X_{\text{H}_2} + X_{\text{OH}} + X_{\text{H}} = \text{ae.XE} \quad \dots (108)$$

$$\text{Oxygen: } X_{\text{H}_2\text{O}} + X_{\text{OH}} + X_{\text{NO}} + 2X_{\text{O}_2} + X_{\text{O}} = \text{ae.LE} \quad \dots (109)$$

$$\text{Nitrogen: } 2X_{\text{N}_2} + X_{\text{NO}} + X_{\text{N}} = \text{ae.ZE} \quad \dots (110)$$

From equation (89), the following relationships are obtained;

$$\text{LE} = 1 + \frac{6}{f} \quad \dots (111)$$

$$\text{WE} = 2 \quad \dots (112)$$

$$\text{XE} = 6 \quad \dots (113)$$

$$\text{ZE} = \text{LE} \frac{78}{21} \quad \dots (114)$$

$$\text{VE} = \frac{1}{2} \cdot \text{LE} \cdot \frac{1}{21} \quad \dots (115)$$

Values of (ae) and (b) were calculated as follow [6];

Value of (ae)

When  $f \geq 1.0$

$$\text{ae} = \frac{1.3}{[\text{WE} + 0.5 \cdot \text{XE} + 1.863(2\text{WE} + 0.5 \cdot \text{XE})/f] \cdot \exp\left(\frac{0.13T}{1000}\right)} \quad \dots (116)$$

and when  $f < 1.0$

$$\text{ae} = \frac{1.3}{[0.25 \cdot \text{XE} + 2.363(2\text{WE} + 0.5 \cdot \text{XE})/f] \cdot \exp\left(\frac{0.13T}{1000}\right)} \quad \dots (117)$$

Value of (b)

$$\text{Whene temperature } T > 3000 \text{ K} \quad \dots (118)$$

$$b = \exp(10.3 - (3.1 - 0.17 \log(P)) \cdot T/1000) \quad \dots (119)$$

and when  $T \leq 3000$  K

$$b = \exp(-9.0 - 0.5 \log(P) + 30000/T) \quad \dots (120)$$

Adjust (b) for the following case

$$BX = 2.0 - 9.0 \log(f) \quad \dots (121)$$

If  $BX > 3.5$ ,

$$BE = \exp(\exp(3.5) + 0.25 \log(P)) \quad \dots (122)$$

If  $BX \leq 3.5$ ,

$$BE = \exp[\exp(2.0 - 9.0 \log(f)) + 0.25 \log(P)] \quad \dots (123)$$

If  $b > BE$ , then use

$$b = BE \quad \dots (124)$$

To evaluate the above 12 mole fractions, the following procedure is used.

Using equations (97), (101), (104) and (108) the mole fraction of hydrogen is obtained;

$$X_{H_2} = \left[ -\left( \frac{KP5}{\sqrt{P}} b + \frac{KP1}{\sqrt{P}} \right) + \sqrt{\left( \frac{KP5}{\sqrt{P}} b + \frac{KP1}{\sqrt{P}} \right)^2 + 4(2b + 2)ae.XE} \right] \frac{1}{4(b + 1)} \quad \dots (125)$$

From equation (104) the mole fraction of water vapor is obtained;

$$X_{H_2O} = b \cdot X_{H_2} \quad \dots (126)$$

and from equation (101) the mole fraction of hydroxyl is obtained;

$$X_{OH} = \frac{KP5b\sqrt{X_{H_2}}}{\sqrt{P}} \quad \dots (127)$$

From equation (97) the mole fraction of atomic hydrogen is obtained;

$$X_H = \frac{KP1\sqrt{X_{H_2}}}{\sqrt{P}} \quad \dots (128)$$

Using equations (99), (103) and (110) the mole fraction of nitrogen is obtained;

$$X_{N_2} = \left[ \frac{-\left( \frac{KP7}{\sqrt{P}}b + \frac{KP3}{\sqrt{P}} \right) + \sqrt{\left( \frac{KP7}{\sqrt{P}}b + \frac{KP3}{\sqrt{P}} \right)^2 + 8aeZE}}{4} \right]^2 \quad \dots (129)$$

From equation (99) the mole fraction of atomic nitrogen is obtained;

$$X_N = \frac{KP3\sqrt{X_{N_2}}}{\sqrt{P}} \quad \dots (130)$$

and from equation (103) the mole fraction of nitric oxide is obtained;

$$X_{NO} = \frac{KP7b\sqrt{X_{N_2}}}{\sqrt{P}} \quad \dots (131)$$

and from equation (100) the mole fraction of oxygen is obtained;

$$X_{O_2} = \frac{KP4b^2}{P} \quad \dots (132)$$

From equation (98) the mole fraction of atomic oxygen is obtained;

$$X_O = \frac{KP2\sqrt{X_{O_2}}}{\sqrt{P}} \quad \dots (133)$$

By using equations (102) and (107) the mole fraction of carbon dioxide is obtained;

$$X_{CO_2} = \frac{aeWE}{\left[ \frac{KP6}{b} + 1 \right]} \quad \dots (134)$$

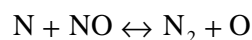
From equations (107) the mole fraction of carbon monoxide is obtained;

$$X_{CO} = aeWE - X_{CO_2} \quad \dots (135)$$

Finally from equation (106) the mole fraction of argon is obtained;

$$X_{Ar} = aeVE \quad \dots (136)$$

The calculations were based on the equilibrium assumption except for NOx formation where the extended Zeldovich mechanism was used.



$$K1f = 3.1 \times 10^{10} \exp\left(\frac{-160}{T}\right) \quad \dots (137)$$



where  $K_{if}$  denotes the forward rate constant for the  $i$ th reaction.

Let  $K_{ib}$  the backward rate constant for the  $i$ th reaction and  $R_i$  equilibrium rate for the  $i$ th reaction.

Then,

$$a_{NO} = \frac{[NO]}{[NO]_e} \quad \dots (140)$$

$$b_N = \frac{[N]}{[N]_e} \quad \dots (141)$$

From equation (137), the net rate is;

$$-K_1 f [N][NO]_e K_1 b [N_2][O] = -a_{NO} \cdot b_N [N]_e [NO]_e K_1 f + K_1 b [N][O]_e \quad \dots (142)$$

and

$$K_1 f [N]_e [NO]_e = K_1 b [N_2]_e [O]_e = R_1 \quad \dots (143)$$

so that the net rate becomes

$$-a_{NO} \cdot b_N \cdot R_1 + R_1 \quad \dots (144)$$

Using the similar terms for equations (138) and (139), involving NO, then;

$$\frac{1}{[NO]_e} \cdot \frac{d([NO]_e \cdot Ven)}{dt} = -a_{NO} (b_N \cdot R_1 + R_2 + R_3) + R_1 + b_N (R_2 + R_3) \quad \dots (145)$$

Also using equations (137), (138) and (139) the following relationship is obtained;

$$\frac{1}{[N]_e} \cdot \frac{d([N]_e \cdot Ven)}{dt} = -b_N (a_{NO} \cdot R_1 + R_2 + R_3) + R_1 + a_{NO} (R_2 + R_3) \quad \dots (146)$$

It has been found that the relaxation times for equation (146) are several order of magnitudes shorter than that of equation (145) [6]. Therefore, steady state may be assumed for  $[N]$  which means the right-hand sides of equation (146) can be set equal to zero, therefore;

$$b_N = \frac{R_1 + a_{NO} (R_2 + R_3)}{a_{NO} \cdot R_1 + R_2 + R_3} \quad \dots (147)$$

Substituting equation (147) in equation (145), gives;

$$\frac{1}{\text{Ven}} \cdot \frac{d([\text{NO}]\text{Ven})}{dt} = 2(1 - \mathbf{a}^2 \text{NO}) \left[ \frac{\text{R1}}{(1 + \mathbf{a} \text{NO}(\text{R1}/(\text{R2} + \text{R3})))} \right] \quad \dots (148)$$

which is the final rate equation for [NO].

## 4- RESULTS

The mathematical and simulation model has been developed to simulate a four-stroke cycle of a spark ignition engine fueled with ethanol fuel. The model has been applied to the Ricardo E6/US single cylinder research engine. Brief technical data are shown in Table 1.

Table (1): The technical details of the engine.

Type:	Ricardo E6/US, spark ignition engine
Cycle:	Four stroke
Number of Cylinder:	1
Cylinder Bore:	76.2 mm
Stroke:	110.0 mm
Connecting Rod Length:	241.3 mm
Compression Ratio:	variable
Engine Speed:	1500 rpm
Ignition Timing:	variable

The results of the mathematical model were then verified against the experimental data of the engine supplied by the manufacture and the experimental results of other researchers [2-8]. In general a good agreement were obtained between the results predicted by the mathematical model and the experimental results. This verifies that the model developed can be used to a great degree of accuracy.

Figure 6 shows the pressure crank angle diagram for ethanol fuel and the corresponding burned and unburned gas temperature. Figure 7 shows the crank angle diagram of flame front speed and flame front radius. The concentration of the combustion product with the crank angle degrees can be shown in figure 8.

Details of the calculation (figures 6-8) show trends, which have been reported by other workers. This gives confidence in the modeling. The trend of pressure and temperature histories (figure 6) agrees with a number of published results [2,4 and 7]. The increase in flame radius with angle and the variation of flame speed with angle (figure 7) agrees with test results of Benson et al. [6] and Sadiq Al-Baghdadi [7]. The prediction of NO and its relationship to the time for freezing (figure 8) agree well with the work of Norman [4], Benson et al. [6] and Sadiq Al-Baghdadi [8].

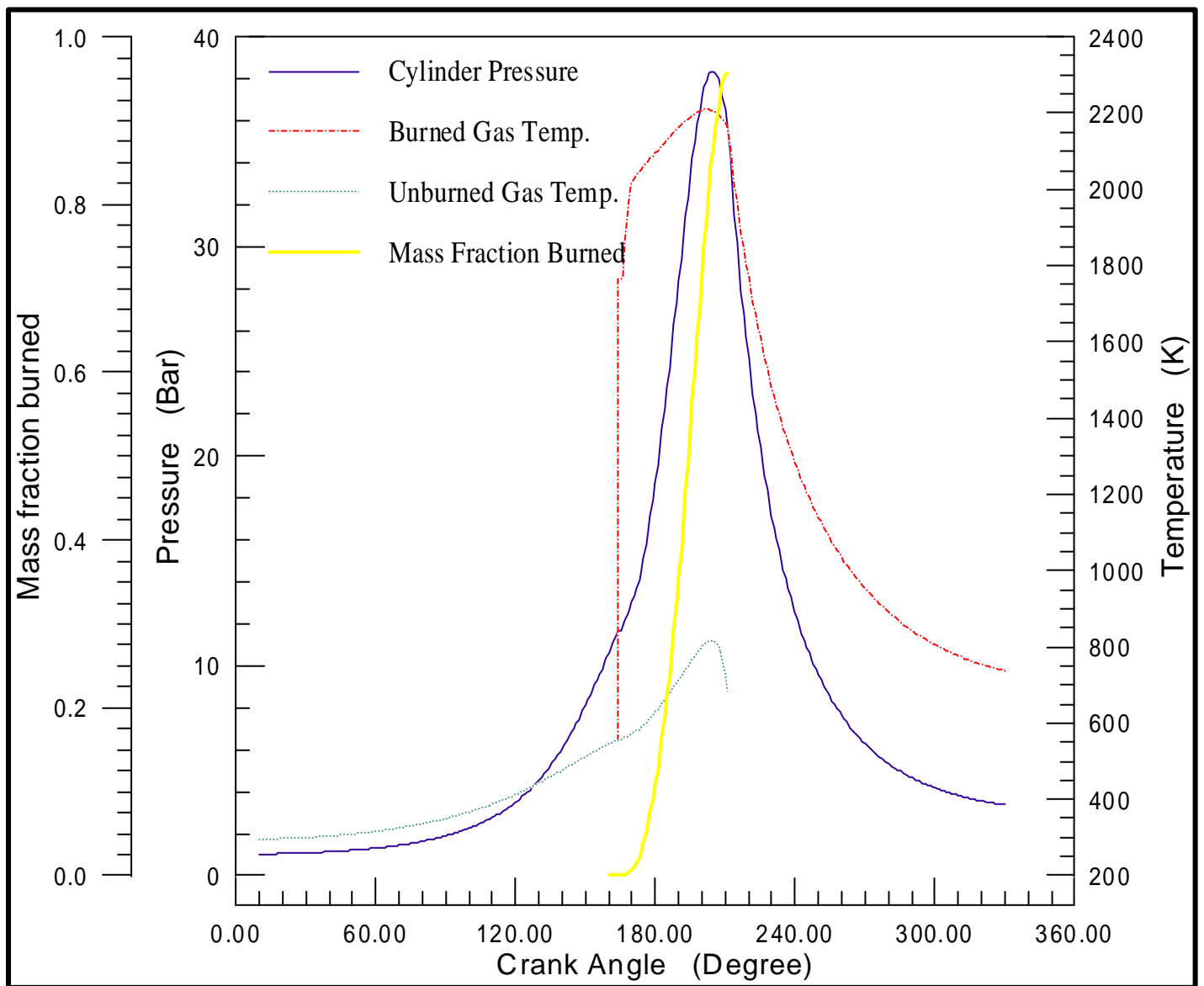


Figure 6: Variation of cylinder pressure, unburned and burned temperature with crank angle. Fuel: ethanol, equivalence ratio: 1, compression ratio: 7.5, engine speed: 1500rpm.

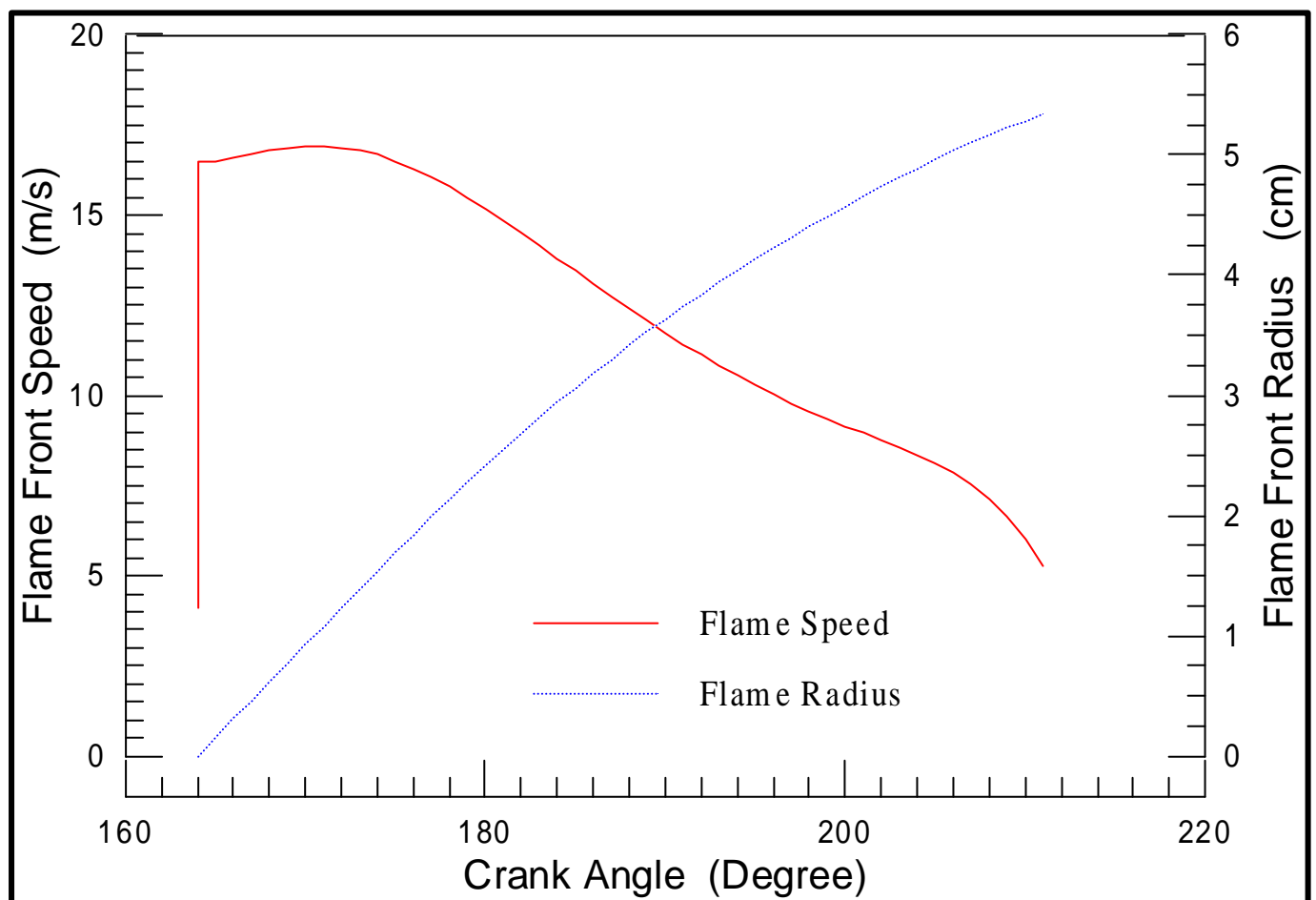
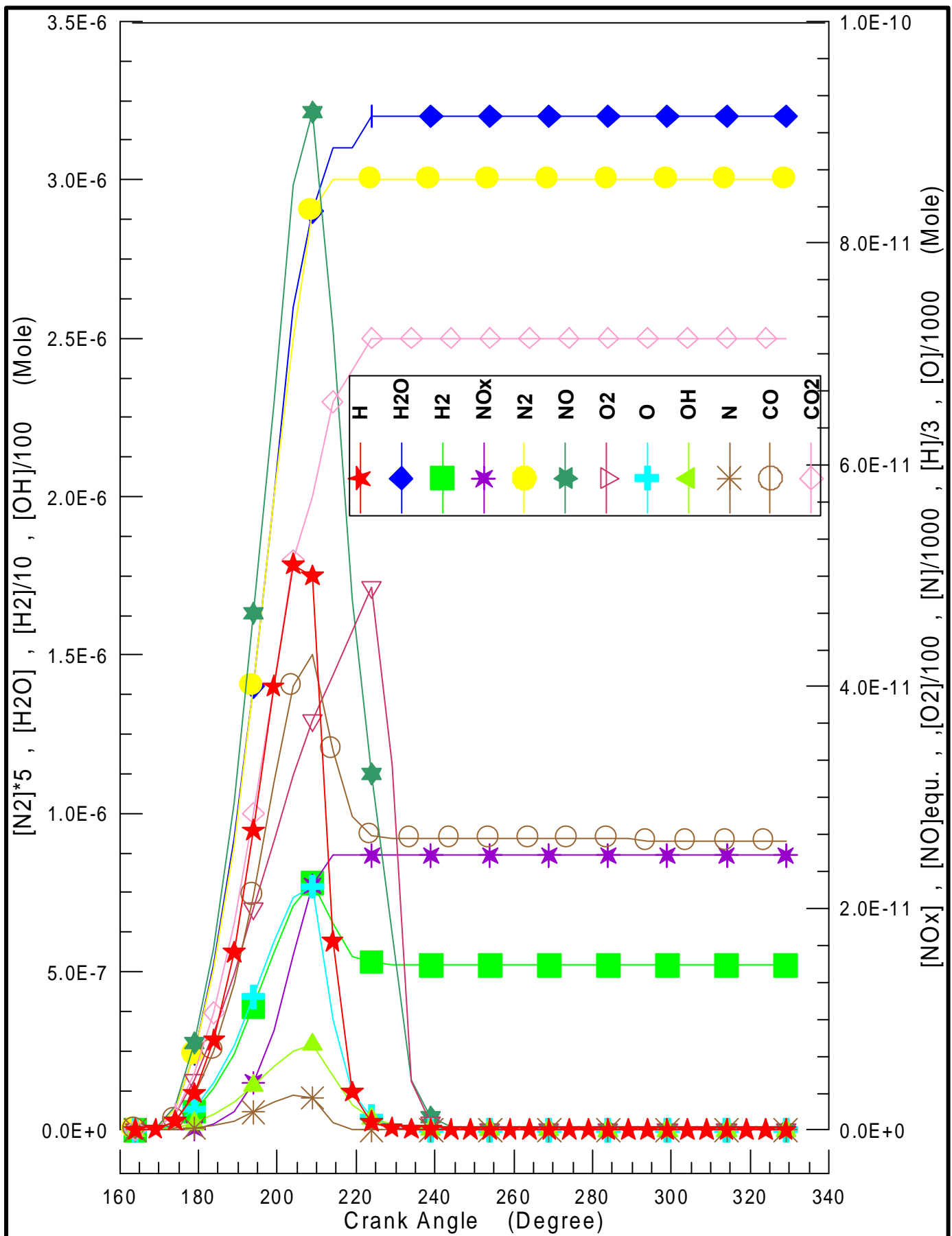


Figure 7: Variation of flame front speed and flame front radius with crank angle.

Fuel: ethanol, equivalence ratio: 1, compression ratio: 7.5, engine speed: 1500 rpm.



## 5- CONCLUSION

The mathematical and simulation model has been developed to simulate a four-stroke cycle of a spark ignition engine fueled with ethanol. The program written from this simulation model can be used to assist in the design of spark ignition engine for alternative fuels as well as to study many problems such as pollutant emissions, catalytic devices, exhaust gas re-circulating valves, effects of misfire and maldistribution of fuel-air mixture, etc.

## REFERENCES

- 1- Heywood J.B. Internal Combustion Engine Fundamentals. McGraw-Hill, 1989.
- 2- Fagelson J.J., Mclean W.J. and De Boer P.C.T. Performance and NOx emissions of spark ignited combustion engines using alternative fuels quasi one dimensional modeling. *Journal of Combustion Science and Technology* 1978; 18,pp.47-57.
- 3- Annand W.J.D.. Geometry of spherical flame propagation in a disc-shaped combustion chamber. *Journal of Mechanical Engineering Science* 1970; 12(2) pp.146-149.
- 4- Norman D. Brinkman. Ethanol fuel-A single- cylinder engine study of efficiency and exhaust emissions. *SAE* 1982; paper no.810345 pp.1410-1424.
- 5- Gatowski J.A., Balles E.N., Nelson F.E., Ekchian J.A. and Heywood J.B. Heat release analysis of engine pressure data. *S.A.E* 1985; paper no.841359 pp.5.961-5.977.
- 6- Benson R.S., Annand W.J.D. and Baruah P.C. A simulation model including intake and exhaust systems for a single cylinder four-stroke cycle spark ignition engine. *Int. J. Mech. Sci.* 1975; 17, pp.97-124.
- 7- Al-Baghdadi Maher. A. Sadiq. Performance study of a four-stroke spark ignition engine working with both of hydrogen and ethyl alcohol as supplementary fuel. *Int. J Hydrogen Energy* 2000; 25(10) pp.1005-1009.
- 8- Al-Baghdadi Maher. A. Sadiq. The safe operation zone of the spark ignition engine working with dual renewable supplemented fuels (hydrogen + ethyl alcohol). *Renewable Energy Journal* 2001; 22(4) pp.579-583.